

Innovative MEMS Voltage-to-Frequency Converter using Cascaded Transducers

Amir J. Majid

Ajman University of Science & Technology, College of Engineering
POB 2202, Fujairah, UAE

ABSTRACT

Voltage-to-frequency (v/f) is often used in communication applications such as tuning circuits and FM systems. With the wide range of Tx/Rx IC devices used in wireless telemetry, as well as the shrinkage of their sizes; a MEMS v/f converter is proposed by implementing multi-stage MEMS sensors and actuators of different types, such as voltage-to-force, force-to-pressure, pressure-to-capacitance and an appropriate capacitance tunable circuit to generate a pulse train of frequency.

Keywords: MEMS, sensors, actuators, transducers, v/f

1. INTRODUCTION

The function of a voltage-to-frequency converter (VFC) [1] is to accept an analog voltage input V_i and generates a pulse train with frequency f , where

$$F = k V_i \quad (1A)$$

K_1 is the VFC sensitivity in Hertz/Volt.

It can be noted that VFC also provides a single form of analog-to-digital conversion in MEMS [2][3][4], in which a pulse train can be transmitted and decoded much more accurately than an analog signal, especially if the transmission path is noisy.

They can provide a voltage-controlled oscillation function (VCO) too, by the use of a suitable tunable circuit. Moreover, combining a VFC with a binary counter and digital readout provide a low-cost digital voltmeter for measurement purposes in wide range of MEMS applications.

The frequency-to-voltage converter (FVC) performs the inverse operation, namely, it accepts a periodic waveform of frequency f_i and yields an analog output voltage V , where

$$V = k F_i \quad (1B)$$

K in this case, is the FVC sensitivity in Volt per Hertz.

FVCs find applications in frequency meters, rotational measurement and digital servo and tachometers [5][6]. They are used in conjunction with VFCs to convert the transmitted pulse train back to an analog voltage.

Electrical isolation and signal transmission can also be achieved without loss of accuracy using opto-couplers or pulse transmission as shown in Fig. (1)

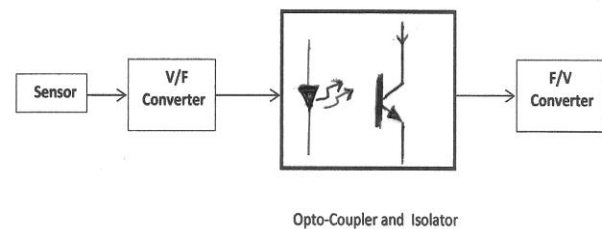


Figure (1) Electrical Isolation and Transmission

2. CASCADED TRANSDUCERS

MEMS sensing and actuating utilizes many basic methods such as electrostatic, thermal, Piezoresistive, Piezoelectric and magnetic [7][8]. The choice of individual method depends primarily on sensitivity, rapid response, simplicity of material, elimination of moving parts, self-generating with no power necessary; among other factors.

Thus, it is possible to use more than one transducer connected in cascade to achieve advantage of some of the above mentioned methods on the expense of other methods.

In the case of v/f and f/v transducers, innovative components for integrated circuitry, including radio frequency (RF) communication chips are required. Examples include micro machined relays, tunable capacitors, resonators and filters. On the other hand,

scaling laws from one physical category to another has to be observed.

In this work, it has been proposed to convert voltage to transverse force or motion, force to pressure and pressure to RF resonance as shown in Fig. (2)

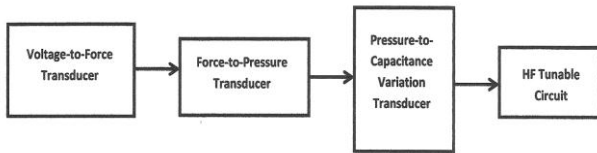


Figure (2) Cascaded Transducers

3. VOLTAGE TO MOTION TRANSDUCER

In a piezoelectric crystal, the constitutive equation [8][9][10] that relates electrical polarization D and applied mechanical stress T is

$$D = dT + \epsilon E \quad (2)$$

Where d is the piezoelectric coefficient matrix, ϵ the electrical permittivity matrix, and E the electrical field. Here, an electric field is applied in conjunction with the mechanical stress to provide more generality. The electrical polarization is contributed by two parts; one stemming from electrical biasing and one from mechanical loading of different orientation in the x , y and z axes. Therefore, The direction of positive polarization is customarily chosen to coincide with the z -axis, whereas T_i a 6-element vector, has six components in which the normal stress components along axes x , y and z are denoted by subscripts 1,2 and 3, respectively, and the shear stress and strain components about these axes are denoted scripts 4, 5 and 6, respectively.

E_i and D_j are both 3-element vectors. Consequently, d_{ij} is a [3X6] piezoelectric constants; in Columb/Newton, and ϵ_{ij} is a [3X3] permittivity matrix in Farad/m. The units of electrical displacement D_i , electrical field E_j and stress T_j and permittivity ϵ_{ij} are Columb/m², Voltage/m, Newton/m² and F/m respectively.

The inverse effect of piezoelectricity can be similarly described by a matrix-form constitutive equation. In this case, the total strain is related to both the applied electric field and any mechanical stress, according to

$$s = ST + dE \quad (3)$$

Where s is a 6-element strain vector and S is 6X6 compliance matrix

3.1 Piezoelectric Force Transducer Model

A model of the deflection of a two-layer piezoelectric structure made of two layers [11][8]; one elastic and one piezoelectric, joined along one side as shown in Fig. (3).

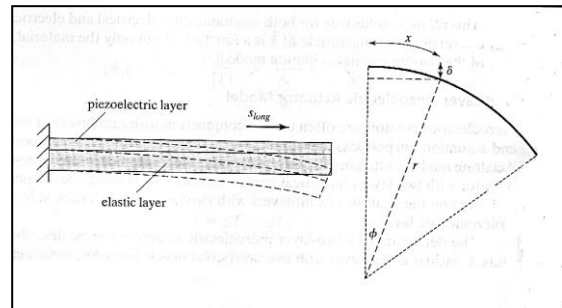


Figure (3) Bending of a piezoelectric bimorph

The beam bends into an arc when the piezoelectric layer is subjected to a longitudinal strain S_1 , in which the radius of curvature can be found to be:

$$r = [\alpha] / [\beta] \quad (4)$$

Where

$$[\alpha] = 4(E_p I_p + E_c I_c)(A_p E_p + A_c E_c) + (A_p E_p A_c E_c)(t_p + t_c)^2$$

$$[\beta] = 2S_1(t_p + t_c)(A_p E_p A_c E_c)$$

A_p , A_c are the cross sectional areas of the piezoelectric and elastic layers

E_p , E_c are the Young's modulus of the piezoelectric and elastic layers

t_p , t_c are the thickness of the piezoelectric and elastic layers. S_1 is the longitudinal strain, which in this case is equal to single element strain

$$S_1 = s_1 = d_{31} E_3 \quad (5)$$

This radius of curvature can be converted to a vertical displacement δ at any location x along the curvature of the cantilever as shown in Fig. (3) according to:

$$\delta(x) = r(1 - \cos(\Phi)) \quad (6)$$

Considering the longitudinal stress (T_1) only, then the strain S_1 and **therefore**, displacement can be approximated as

$$\delta(x) \approx x^2 / 2r \quad (7)$$

Note that only s_1 and consequently d_{31} is considered. Also, the amount of force achievable at the free end of a piezoelectric bimorph model equals the force required to restore the tip of the actuator to its initial undeformed

state. This force is linearly proportional with displacement, i.e.

$$F = k \delta(x=L) \tag{8}$$

k here is a constant of proportionality.

3.2 Vertical Sensor-Actuator Model

Semiconductor materials, which are often used in MEMS circuits, can be made to yield similar piezoelectric characteristics, such as Quartz and ZnO [12][13][14]. Thus, sensors and actuators models of Silicon and Germanium materials are considered.

A patch of ZnO thin film of length A, sandwiched by two electrodes, is located near the base of a cantilever beam, as shown in Fig. (4).

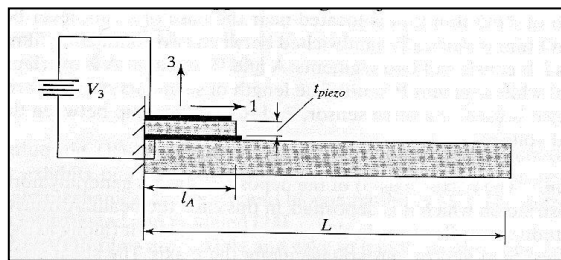


Figure (4) A Piezoelectric force sensor

The length of the beam is l, in which part of it; l_A is overlapped with a piezoelectric ZnO, while l_B is not.

As voltage V is applied between the vertical electrodes length(l_A), an electrical field E and polarization D are produced as

$$E_3 = V/t_p \text{ and } D_3 = \epsilon E_3 \tag{9}$$

This field is mainly a longitudinal one which produces a longitudinal tensile stress s_1 as depicted in equation (5).

Segment A is curved into an arc. The radius of the curvature r due to the applied voltage can be found as

$$r = [\alpha/\beta] d_{31} E_3 / s_1 \tag{10}$$

The displacement at the end of segment A can be found from the angular displacement at the end of the piezoelectric patch $\Phi_A = l_A/r$

The rest of the beam length does not curl and remains straight. The vertical displacement at the end of the beam (l) is:

$$\delta = \delta_A + (l-l_A) \text{Sin}(\Phi_A) \tag{11}$$

3.3 Horizontal Sensor-Actuator Model

The patch of ZnO thin film located on a cantilever is biased by coplanar electrodes, as shown in Fig. (5) [15][14][8].

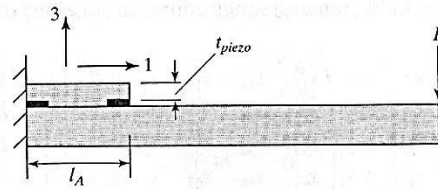


Figure (5) A Piezoelectric actuator

A voltage V is applied across the longitudinal direction, which produces an electric field

$E_1 = V/l_A$. This field creates a longitudinal strain along the beam axis as

$$s_3 = d_{33} E_3 \tag{12}$$

The vertical displacement can be calculated in a similar manner as shown before in equation (11)

4. RESONANCE MODE PRESSURE ACTUATOR

The purpose of this transducer [16][17][18] is to convert displacements due to force or pressure to wireless frequency modulation signals which has the advantage of noise immunity. A pressure sensitive membrane is covered with a spiral planar winding or inductor, which forms a capacitor with an opposite electrode as shown in Fig. (6).

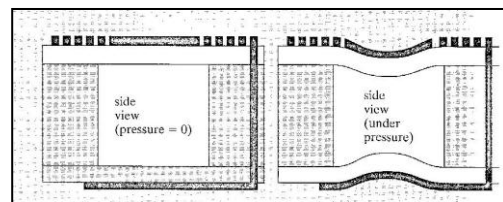


Figure (6) Pressure sensor using RF resonance

If pressure or force changes, the membrane displaces, changing the relative capacitance value. The resonance frequency of the resonant circuit is related to displacement as:

$$C = C_0 \sum_{i=0}^{\infty} \frac{1}{2i+1} \left(\frac{2d_0}{t_g + 2t_m \epsilon_r^{-1}} \right)^i \tag{13}$$

Where C_0 is the capacitance at zero pressure or displacement, d_0 the displacement of the membrane under pressure, t_g and t_m are the size of the gap and the thickness of the membrane, and ε_r is the relative dielectric constant of the membrane.

It can be deduced that an approximation of the capacitance change related to displacement is $\Delta C \approx 2d_0/[3(t_g + 2t_m \Delta C_r^{-1})]$ (14)

It is to be noted that displacement d_0 is related to the deflection $\delta(x)$.

5. RADIO FREQUENCY RESONATOR

Tuning circuit of a transceiver-receiver circuit can be altered by changing the value of the capacitor connected either in series or parallel. This can be accomplished by connecting the resonance mode pressure actuator revised above with a crystal tuning electronic circuit as shown in Fig. (7). Crystals have very stable frequency and are small noise and temperature variations, with frequencies up to 100MHz

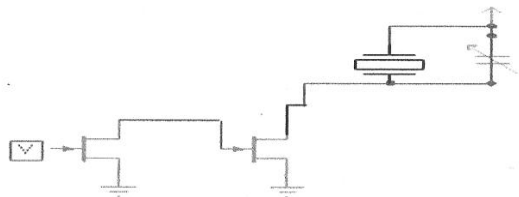


Figure (7) Variable Capacitor Tuning Circuit

There is a problem, though, of smaller frequency variation used in FM applications. This can be remedied by starting with a low resonant frequency crystal and using a frequency multiplier to increase both working frequency and deviation.

6. SIMULATION OF DESIGN EXAMPLES

The following design example is used to simulate the MEMS VFC using MATLAB. A 500µm long cantilever piezoelectric actuator is made of two layers; a ZnO layer and a polysilicon layer as shown in Fig. (8). The width, thickness and material properties are 20µm, 1µm, Young modulus 160GPa, Piezoelectric coefficient 5×10^{-12} pC/N, for the ZnO layer and 20µm, 2µm, 160GPa for the polysilicon. Applied voltage is 10V.

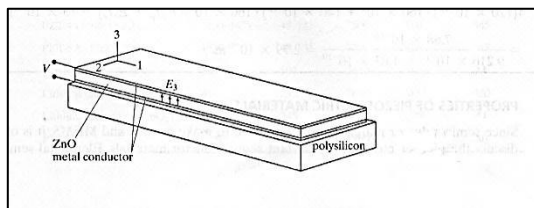


Figure (8) Simulation of a Beam Cantilever

Therefore, $\delta(x=L) = 2.8 \times 10^{-6}$ m

Table (1) depicts displacements for a set of applied voltages ranging 1V-10V at different distances x of 25%, 50%, 75% and 100% of cantilever length.

Table (1) Displacements at four cantilever distances with three applied voltages

| | 25% Length | 50% Length | 75% Length | 100% length |
|-----|-----------------------|----------------------|------------------------|----------------------|
| 1V | 1.75×10^{-8} | 0.7×10^{-7} | 15.75×10^{-8} | 2.8×10^{-7} |
| 5V | 8.75×10^{-8} | 3.5×10^{-7} | 78.75×10^{-8} | 1.4×10^{-6} |
| 10V | 1.75×10^{-7} | 0.7×10^{-6} | 15.75×10^{-7} | 2.8×10^{-6} |

ΔC can be calculated according to t_g, t_m, ϵ_r and the above calculated displacements.

7. CONCLUSION

A MEMS VFC is proposed using voltage-deviation, deviation-capacitance and capacitance-frequency sensors; all based on MEMS principle. This transducer is useful in FM transmission and receiving of sensor signals.

Both longitudinal and transverse forces of the transceiver are considered. It was assumed that ideal material properties are conformed, but this has yet to be investigated in larger details.

Material such as piezoelectric, Quartz and ZnO can be used with diverse material constants.

A 1MHz resonant frequency crystal is proposed to be used with this transducer in an electronic circuit, with the aid of frequency multiplication. A demonstration example is presented at the end.

It is assumed that a MEMS FVC will follow this work in order to confine the functionality of a transmitter-receiver MEMS device.

REFERENCES

- [1] Zumbahlen; Linear Circuit Design Handbook, a book, Newnes, PP. ,2008
- [2] Majid; Electrostatic and Electromagnetic Fields For MEM AD/DA Converters; International Journal of Engineering IJE, Volume 2, Issue 1, February 29th 2008
- [3] Majid; Modeling MEMS with MATLAB’s SIMULINK; International Conference on Modeling, Simulation and Applied Optimization, ICMSAO 2007, PI, Abu Dhabi, March 24-27 2007
- [4] Majid, Electrostatic and Electromagnetic Fields For MEM AD/DA Converters; International Journal of Engineering IJE, Volume 2, Issue 1, February 29th 2008

- [5] Li, et al., Fabrication of a High Frequency Piezoelectric Microwave Sensors and Actuators, Physical 111, PP.51-56, 2004
- [6] Hall, Degertekin; Integrated Optical Interferometric Detection Method for Micromachined Capacitive Acoustic Transducers; Applied Physics Letters, 80, pp.3859-3861, 2002
- [7] Gabrielson; Mechanical-Thermal Noise in Micromachined Acoustic and Vibration Sensors; Electron Devices IEEE Transaction, 40, pp.100-114, 1999
- [8] Chang Liu; Foundations of MEMS, a book, Prentice Hall, pp. ,2006
- [9] Toriyama and Sugiyama; Analysis of Piezoresistance in p-type Silicon for Mechanical Sensors; MEMS Journal, 11, pp. 598-604, 2002
- [10]Muralt; Ferroelectric Thin Films for Microsensors and Actuators; Journal of Micromechanical and Microengineering, 10, PP. 136-146, 2000
- [11]Yaralioglu, et al., Analysis and Design of an Interdigital Cantilever as a Displacement Sensor; Journal of Applied Physics, 83, pp. 7405-7415, 1998
- [12]Maier-Schneider, Maibach and Obermeier; A New Analytical Solution for the Load-Deflection of Square Membranes; MEMS System Journal, 4, pp. 238-241, 1995
- [13]Tadmor, Kosa; Electromechanical Coupling Correction for Piezoelectric Layered Beams; MEMS Journal, 6, PP. 899-906, 2003
- [14]Elka, Elata, Abramovich; The Electromechanical Response of Multilayered Piezoelectrical Structures; MEMS Journal, 13, PP. 332-341, 2004
- [15]Kuoni, et al.; Polyimide Membrane with ZnO Piezoelectric Thin Film Pressure Transducers as a Differential Pressure Liquid Flow Sensor; Journal of Micromechanics and Microengineering, 13, pp. S103-S107, 2003
- [16]Inagaki, Shimizu; Resource Conservation of Buffered HF in Semiconductor Manufacturing; Semiconductor Manufacturing IEEE Transactions, 15, PP. 434-437, 2002
- [17]Annovazz—Lodi, Merlo, Norgia; Comparison of Capacitive and Feedback Interferometric Measurements on MEMS; MEMS Journal, 10, pp. 327-335, 2001
- [18]Fonseca, et al., Wireless Micromachined Ceramic Pressure Sensor for High Temperature Applications, MEMS Journal 11, pp. 337-343, 2002